EVALUATION OF DIE WEAR IN WIRE DRAWING USING RADIO-TRACERS

By

SRIVALLABH JAJOO

DEPARTMENT OF MECHANICAL ENGINEERING

INDIAN INSTITUTE OF TECHNOLOGY, KANPUR

MARCH, 1979

EVALUATION OF DIE WEAR IN WIRE DRAWING USING RADIO-TRACERS

A Thesis Submitted
In Partial Fulfilment of the Requirements
for the Degree of
MASTER OF TECHNOLOGY

By
SRIVALLABH JAJOO

to the
DEPARTMENT OF MECHANICAL ENGINEERING
INDIAN INSTITUTE OF TECHNOLOGY, KANPUR
MARCH, 1979

ME-1979-M-JAJ-EVA

CERTIFICATE

This is to certify that this work entitled, 'EVALUATION OF DIE WEAR IN WIRE DRAWING USING RADIO-TRACERS' by Shri Srivallabh Jajoo has been carried out under our supervision and has not been submitted elsewhere for a degree.

(G.K. Lal)
Professor
Mechanical Engg.Dept.
IIT Kanpur

(K. Sri Ram)
Professor and Convener
Nuclear Engg. Programme
Indian Institute of Tech.,
Kanpur

Dedicated

to

MAMA AND MAMI

ACKNOWLEDGEMENTS

I wish to express my deep sense of gratitude to Professors K. Sri Ram and G.K. Lal for their constant encouragement, enlightening guidance and inexhaustible patience observed by them throughout the course of my thesis work.

I would like to thank Dr. R. Chawla for suggesting the problem and helping me in the initial stages.

I acknowledge with thanks the invaluable cooperation and timely help received from Harish and Deva Datta. I owe my thanks to all my friends who made my life enjoyable and helped me in more than one way throughout my stay at IIT Kanpur.

I am thankful to Mr. Chakravarty, Works Manager of Arkay Wires, Kanpur for his help at various stages, to M/S Ghewar Chand and Sons, Jaipur for manufacturing the HSS die to desired specifications.

Sincere thanks are due to many people at IIT/Kanpur- in particular, to Messrs R.M. Jha, B.P. Viswakarma, Joginder Singh, S.S. Pathak and all the lab. staff for the engineering support, to Mr. A.K. Ganguly for tracing work, to Mr. J.K. Misra for excellent typing and to Buddhi Ram and Panditji for cyclostyling.

Financial assistance is gratefully acknowledged from the Department of Science and Technology, Govt. of India, under whose sponsorship this work was carried out.

Last but not the least, I owe my heartfelt thanks to Uma for giving me moral support during the last stages of my work.

March , 1979 Vallabh

CONTENTS

LIST OF FIGURES

SYNOPSIS

Various radio-tracer methods have been used in the past for the study of wear in metal cutting and metal forming. Of them γ-γ coincidence technique has proved quite successful in the study of machining. Here the same technique has been used to study die wear and its success has been established as also its efficacy over conventional methods.

Wire drawing experiments were carried out on irradiated HSS (active isotope Co^{60}) dies using MS wire. The activity of drawn wire samples at the known lengths was measured by a γ-γ coincidence set-up and the absolute volumetric wear was calculated.

Volumetric wear and inverse wear rate curves were plotted for different speeds. These curves resemble those obtained for single point tool wear. Thus it seems reasonable that die life equation similar to tool life equation can be obtained. The built up edge effect was observed at lower speeds similar to that in machining. For the dies considered force variations were found to be insignificant. HSS dies were found to have higher frictional coefficients than Carbide dies. It was also found that continuous operation may lead to higher die life.

CHAPTER I

INTRODUCTION

1.1 Introduction:

Wear is generally defined as the progressive loss of substance from the operating surface of a body occurring as a result of relative motion of the surfaces[1].

An important problem of wear which is faced in industry is about tools in general. The tool life equation has been established by making some assumptions and it has been proved theoretically and experimentally as well. Similarly in the wire drawing industry, a die is a precision tool and its life is an important factor. Die life affects production costs in three ways - in down time for die changing, in labour and over heads involved in repolishing the die and in the replacement of dies. The above facts give a way to think about die life and the wear problems which are attached to it.

1.2 Mechanics of Wire Drawing:

Wire drawing has been evolved through experience rather than by the application of scientific principles. The drawing process is shown diagrammatically in Fig.1.1. The wire deforms plastically in the deformation zone and

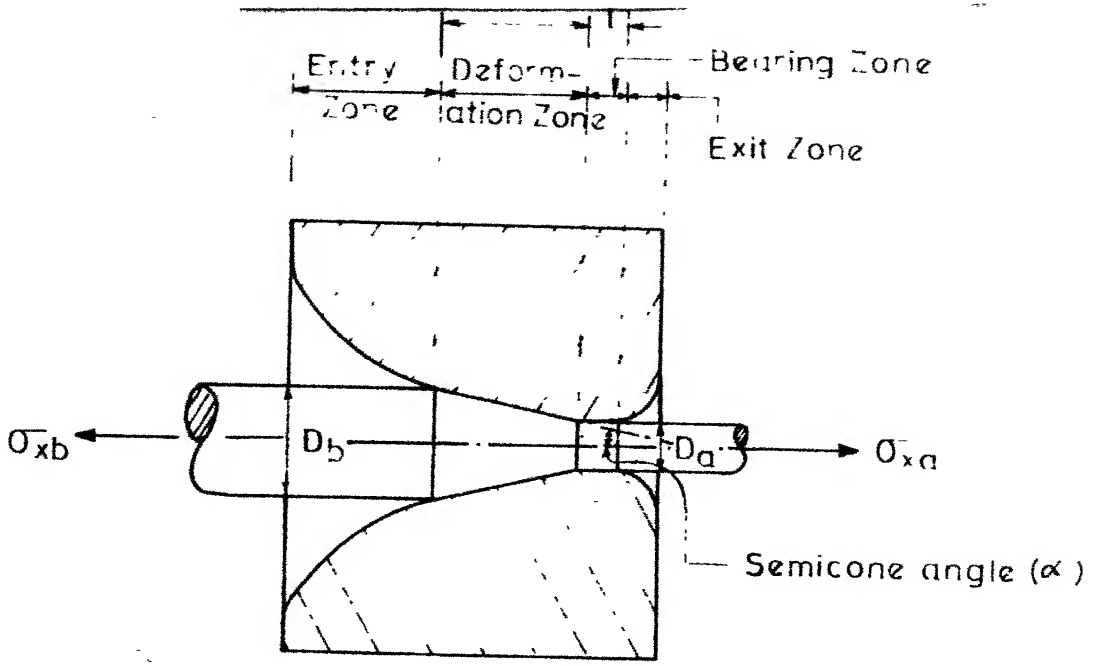

FIG. 1.1 WIRE DRAWING OPERATION

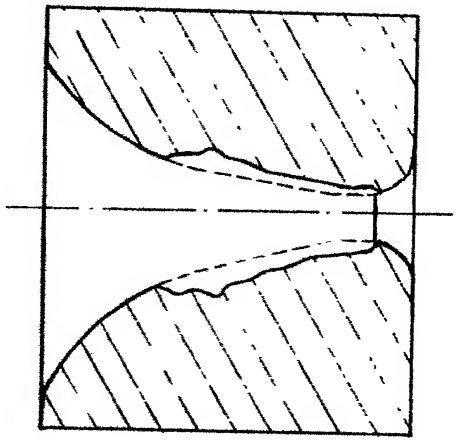

reduction in diameter is achieved. The cylindrical portion of the die, called the bearing zone, is provided for the dimensional stability of the drawn wire, although it results in additional frictional losses.

As the wire passes through the die, there is relative motion between the wire and die surface which causes sliding friction. The mechanism of friction is recognised as the formation and rupture of minute bridges between asperities of sliding surfaces.

Lubricants can be used to separate the sliding surfaces. Theoretical evaluation has been done to study the effect of lubricants by few workers [2,3]. The pressure on the surface of the die and drawing stresses can be calculated assuming a coefficient of sliding friction between the wire and die surfaces. The values for the coefficient of friction can be taken from the results of Wisterich [4] and Yang [5].

In the deformation zone the material reaches plastic state and starts flowing. This plastic formation results in strain hardening and residual stresses. With increase in drawing speed the rate of straining of the material will increase. The level of the flow stress curve tends to increase with increasing rate of strain. The stress-strain curve of the metal is also sensitive to temperature. The

yield stress decreases with increasing temperature [6]. The wire drawing operation is usually carried out at high speeds and therefore, high strain rates are involved in the process. When a material is deformed at a temperature below its recrystallization temperature, it strain-hardens [6]. Alder and Phillips [7] have reported the strain-hardening effects for various materials and calculated the strain-rate sensitivity coefficients for a range of temperature and reduction in area.

Due to frictional heating in the deformation zone with irreversible plastic deformation of the wire material within the deformation zone, the temperature of the material rises. Some of the heat generated will be carried away by the lubricants (if used), while some may dissipate through the casing [8]. Further, if the residence time of the metal in the zone of deformation is sufficiently short (of the order of few micro seconds), the effect of transient temperature rise during deformation may be insignificant and the thermal softening effect within the deformation zone will probably be small as compared to strain-rate effects [9].

Wistreich [4] has reported the effects of reduction of cone angle and area reduction on drawing stress. He has observed significant strain hardening effects. He also

reported in his work on wire drawing that the wire radius contracts at the exit to a size smaller than the die radius. The reason being, wire will be at higher temperature when it is drawn and the temperature will go down as soon as it is exposed to the atmosphere. In this process wire diameter increases after it is drawn.

Due to various combinations of factors (reduction, die angle, friction, properties of material etc.) defects are caused. Due to difficulties mentioned above it is often observed that dies have dead zone formation and on the drawn wire snake skin formation, chevroning, bulging and contraction, shaving etc. Because of the undesirable combination of variables, it is difficult to analyse the wear phenomena.

1.3 Mechanism of Wear:

As is well known, wear is a complex phenomenon that cannot be predicted with any great accuracy. This is because one type of wear usually does not occur in isolation but merely predominates. Further, interactions between different forms of wear also occur. Depending on the nature of movement of media involved in an interaction under load the following types of wear have been classified [10].

Adhesive Wear.

In this, the relative movement can be unidirectional or reciprocating sliding or interaction occurs under small amplitude oscillatory contact load. The mating surface peaks are known to flow plastically and to form strong work hardened junctions. As these break under an imposed tangential traction, material loss from the solids may occur [10].

Abrasive Wear.

Abrasive particles in the form of wear debris or adventitious particles of grit and dust from the surroundings remain trapped at the sliding interface and remove material largely by ploughing [10].

Other Forms of Wear:

Fretting is a form of wear which occurs as a result of oscillatory movement between two surfaces as in machine parts. Fatigue wear arises as a result of cyclic loading. Erosive wear results when grits impinge on solids and cavitation erosion may arise when a component rotates in a fluid medium [10].

The mechanism of wear in wire drawing dies had been studied in the past by means of metallographic examination of the profiles of worn dies, spectrographic analysis of used wire drawing soap (lubricant) and by observing the

dissipation of wear debris attached to the drawn wire and originating from radioactivated dies [11].

It has been observed that the intensity of wear varies along the die surface; it is least in the middle, more at the exit and maximum at the entry. Moreover, the differences in the microscopic appearance of worn die surface at the entry and else where are such that one is led to suspect that a different mechanism of wear is at work at the entry of the die, where a deep and clearly defined annular crater is formed. This is referred to as 'ringing'[11]. A typical worn-out die is shown in Fig.(1.2).

The application of radioactive methods to study die wear have been very rare. Joul [12] has studied die wear (in deep drawing) by activating the surfaces, using the auto-radiograph method. Button et al.[13] studied the wear of wire drawing dies by surface activation method. The experiments were performed on a draw bench. G.M. Counters and auto-radiograph methods were used. The speed of drawing was 22 cm/sec. The wear was of the order of 2×10^{-8} gms/ft length of wire. On line wear monitoring was studied by Askouri et al. [14]. They used activated bearing zone surface upto the depth of 70 μm and had estimated the wear rates for new die and resized die. They found that the new die wore at a steady rate where as the resized die wore at non uniform rates in the bearing zone.

For tungsten carbide dies, Wistreich [11] concluded from the presence of radioactive smudges of cobalt on the wire that microscopic welding occurs between the cobalt matrix of the die and the metal of the wire. The carbide grains are thereby exposed and are polished away, broken or torn out. Some of the carbide particles become embedded in the wire and are probably responsible for the scoring of the die.

1.4 Present Work:

In the present work an attempt has been made to estimate die wear during wire drawing by using γ-γ coincidence technique. This technique has been earlier successfully used for obtaining absolute wear values during single point cutting. Scintillation detectors were used for detection. The work was then extended to study the effect of drawing speed on the volumetric wear of the die.

CHAPTER II

EXPERIMENTAL SET-UP AND TECHNIQUES USED FOR MEASURING WEAR

In this chapter, a discussion of the experimental set-up, techniques used for measuring die wear, measurement of force, evaluation of frictional coefficient etc. is given. Basically the experiment consists of drawing a given wire through a wire drawing machine using a radioactive die and counting sections of the drawn wire for its activity. Details of various components are described below including the set-up for measuring the drawing forces involved in the wire drawing process.

2.1 Experimental Set-up:

2.1.1 Wire Drawing:

The present work has been carried out on a vertical wire drawing machine manufactured by wire machinery manufacturing corporation ltd., Calcutta. The specifications are given in Appendix I.

Preliminary experiments were performed using HSS and Tungsten Carbide dies. Initially it is necessary to point the wire fora certain length, so that it may be passed through the die and gripped by the jaws of a pulling dog. The pulling dog is to be fixed in the holes which are provided on the capstan. When the capstan rotates the

wire is drawn. In the industry a pointing machine is used to point the wire. As the pointing machine was not available various methods were tried. Grinding and filing methods were tried and it was observed that pointed wire will not be of same diameter throughout the length. Due to non-uniformity in diameter wire used in break when the load was applied. The scratching die method was also tried but it too did not work. Finally drawing it through a Tungstan Carbide die (1.85 mm dia. at exit) was tried.

A small portion of wire was first filed and then it was passed through the die. The TC die was held in the lathe tool post with a stopper and the end of the wire was held in the chuck. The carriage was moved away from the head stock. After drawing the wire to a certain length it was pulled back by holding the wire with bolt and nut and stopping it at the tailstock handle. In this way, a uniform diameter pointed wire was obtained. But after this also wire broke when load was applied. The reason being that the wire was not able to take the jerk of the suddenly applied load when the motor was started. It was also decided to use speed of drawing as one of the parameters which effects the wear. The two factors above, the former being the major one, it was necessary to attach a gear box to the machine.

2.1.2 Gear Box Attachment:

A Tata GB-30 gear box, which gives five varying speeds (8, 15, 25, 40, 62.5 rpm corresponding to the five gears) was coupled to the motor. The gear box was fixed on a L-plate, which was properly machined on a milling machine, with the help of bolts and nuts. Two cast iron blocks were cast to make the V-grooved pulley for the drive. As there was no further need to vary the speed, the blocks were machined according to the dimensions of the pulley provided with the 20 HP motor. On one of the pulleys a keyway was cut to fix it on the spline shaft of the gear box and on the other tapped holes were made. The gear box assembly (with L-plate) was fixed on the channels provided. The system was driven by V-belts. Photograph 2.1 shows the attachment.

2.1.3 Spool:

To measure the activity of all the drawn wire is difficult and time consuming process, which defeats one of the main purposes of using this technique. It was decided that samples of 1 m length at various measured distances would be taken. For this purpose a wire winding spool was fabricated of which the drum circumference was known. By noting down the number of revolutions it makes, the exact position of the sample taken may be noted.

2.1.4 Shielding and Other Safety Considerations:

For handling a highly radioactive die it was necessary to make shielding arrangements so that the exposure to persons working with the die is within the safe limits specified by ICRP guide lines (2.5 m rem/hr). After taking all the safety factors into consideration a movable box typ. shield or a trolley which covers the die post completely was found suitable. The time of the radioactive die — handled was also minimized. Lead bricks were used for shielding. The thickness of the shield was calculated using the known activity of the die and the trolley was designed accordingly using a factor of safety of 2 (for the load of bricks). A screw-jack was also fabricated to support the rails when the trolley is completely outside the die box. Photograph 2.2 shows the details.

Other safety measures were also observed. Removable rubber sheets covered the experimental floor area. A set of hand gloves and nose mask were used during the experiments. Film badges were used to know the dosage. After experimentation machine was cleaned and all the loose particles were collected. The activity of the loose particles was measured. It was found that this activity was less than half a percent of the total activity of the wire counted. Machine was surveyed with radiation monitors after complete cleaning. There were no traces of radiation.

2.1.5 Dynamometer:

Here it is necessary to know the variation in drawing forces as wear rate increases, decreases or stabilises. Fig. 2.1 shows an extended octagonal ring by which normal force (T), tangential force (P) and moment (M) can be measured. Strain gauges were mounted on the ring as shown. Three different wheatstone bridge circuits are necessary to measure T, P and M. The deflection due to the drawing forces and strains developed in the ring can be calculated using the following equations (15).

$$\delta_p = 3.7\ Pr^3/Ebt^3$$

$$\varepsilon = 1.4\ Pr/Ebt^2$$

where, P is the drawing force, r the mean radius, b the width and t the thickness of the ring. Further, E is the Young's Modulus, δ_p the deflection and ε the strain.

In the above equations all the parameters are known except drawing force P. This can be calculated using the following equation [16].

$$\frac{\sigma_{xa}}{Y} = \frac{1+B}{B}\left[1-\left(\frac{D_a}{D_b}\right)^{2B}\right] + \frac{\sigma_{xb}}{Y}\left[\frac{D_a}{D_b}\right]^{2B} \qquad (2.1)$$

where $B = \mu \cot \alpha$, μ is the coefficient of friction, α the semicone angle of the die, σ_{xa} the front tension, σ_{xb} the back tension, Y the yield stress, D_a and D_b the diameter of the wire at the exit and entry.

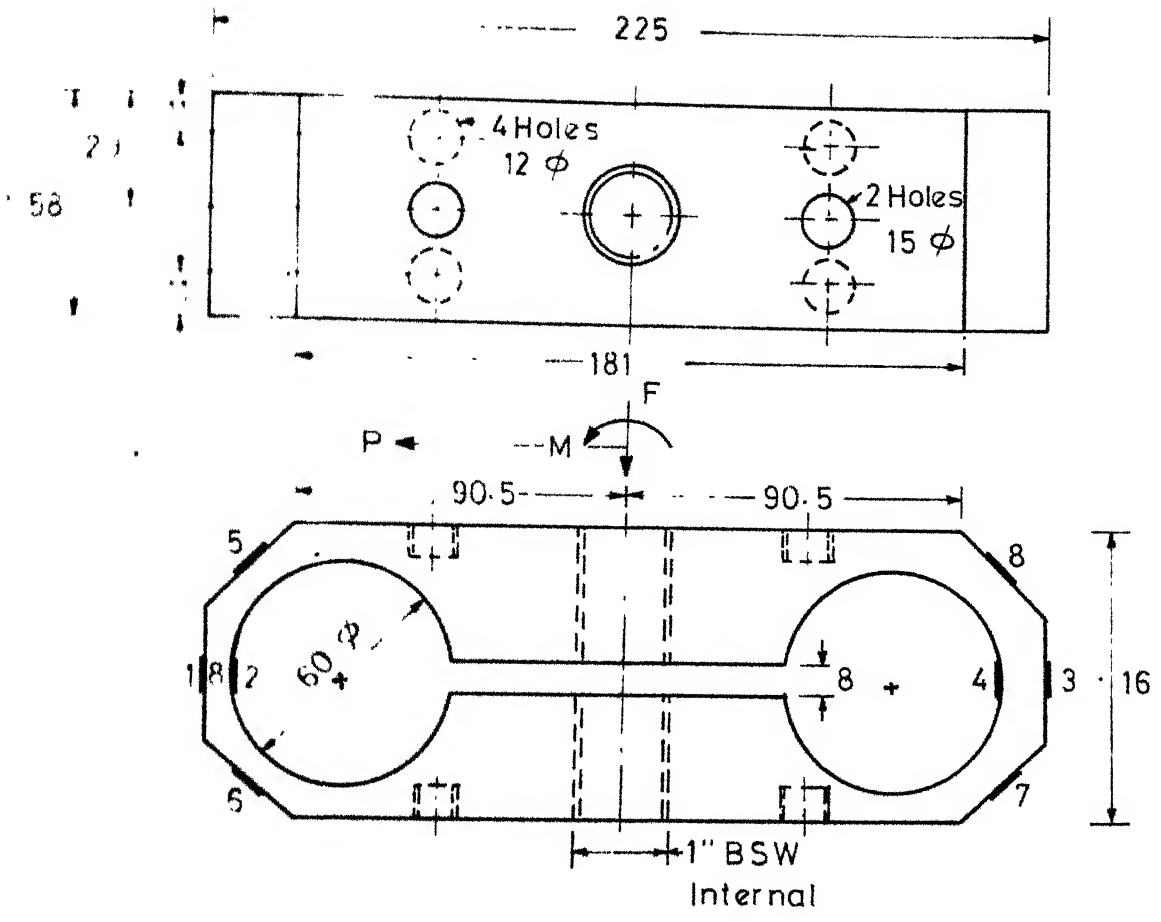

(a) DYNAMOMETER.

Dimensions are in mm

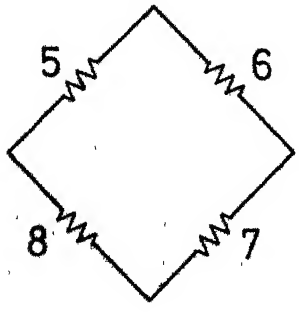

(b) P-Circuit

FIG 2.1 (a) DYNAMOMETER & P-Circuit

... strain σ_{xx} (back tension) = 0

... (2.1) reduces to

$$\frac{\sigma_y}{\sqrt{2}} \left[1 - \left(\frac{D_a}{D_b}\right)^{2B}\right] \qquad (2.2)$$

... the value of yield stress for the wire material and coefficient of friction, drawing stress and ... drawing force can be calculated as also δ_p and strain. By knowing the gauge factor and the excitation voltage the output voltage can be calculated by

$$\text{(output voltage)} = \frac{a}{4} FV\varepsilon \qquad (2.3)$$

where a is the number of strain gauges used, F the gauge factor, V the excitation voltage and ε the strain.

For the range of drawing forces that are expected, it is found from the above equation that the output of the dynamometer is significant and can be recorded accurately on strip chart recorder. As the accuracy needed was high, semiconductor strain gauges were used as they have high gauge factor and resistance.

Semiconductor strain gauges were fixed and the circuit was connected as shown in Fig. (2.1). All the specifications are given in Appendix II. Photograph 2.3 shows the dynamometer and die post mounting on the machine.

2.2 An Encardio-rite strip chart recorder was used for continuous recording of the output of the circuit. The strain gauges were excited by applying 12 V from a standard voltage supply (Aplab). Output terminals were connected to Encardio-rite recorder.

By applying a known load the calibration of the dynamometer was made. The Fig. (2.2) shows the calibration curve. The linearity of the Encardio-rite Recorder response was checked and found that the ranges used in this experiment have a linear relationship.

2.2 Die and Die Materials:

2.2.1 Die Profiles:

In the wire drawing process the die is a precision tool. The successful drawing operation and the die life depends on the die profile. Hu [17] has done the analysis of die profiles on 4 different profiles viz. convex, concave, straight and bell shaped. The bell profiled die has the most uniformly distributed frictional forces along the die. Therefore, it is expected that the wear of the die for bell profiles will be the most uniform. This is the main consideration factor for better efficiency and longer life of the die in wire drawing. But practically speaking bell and convex shaped die production is very difficult. Hence a straight profiled die was chosen for the experiments.

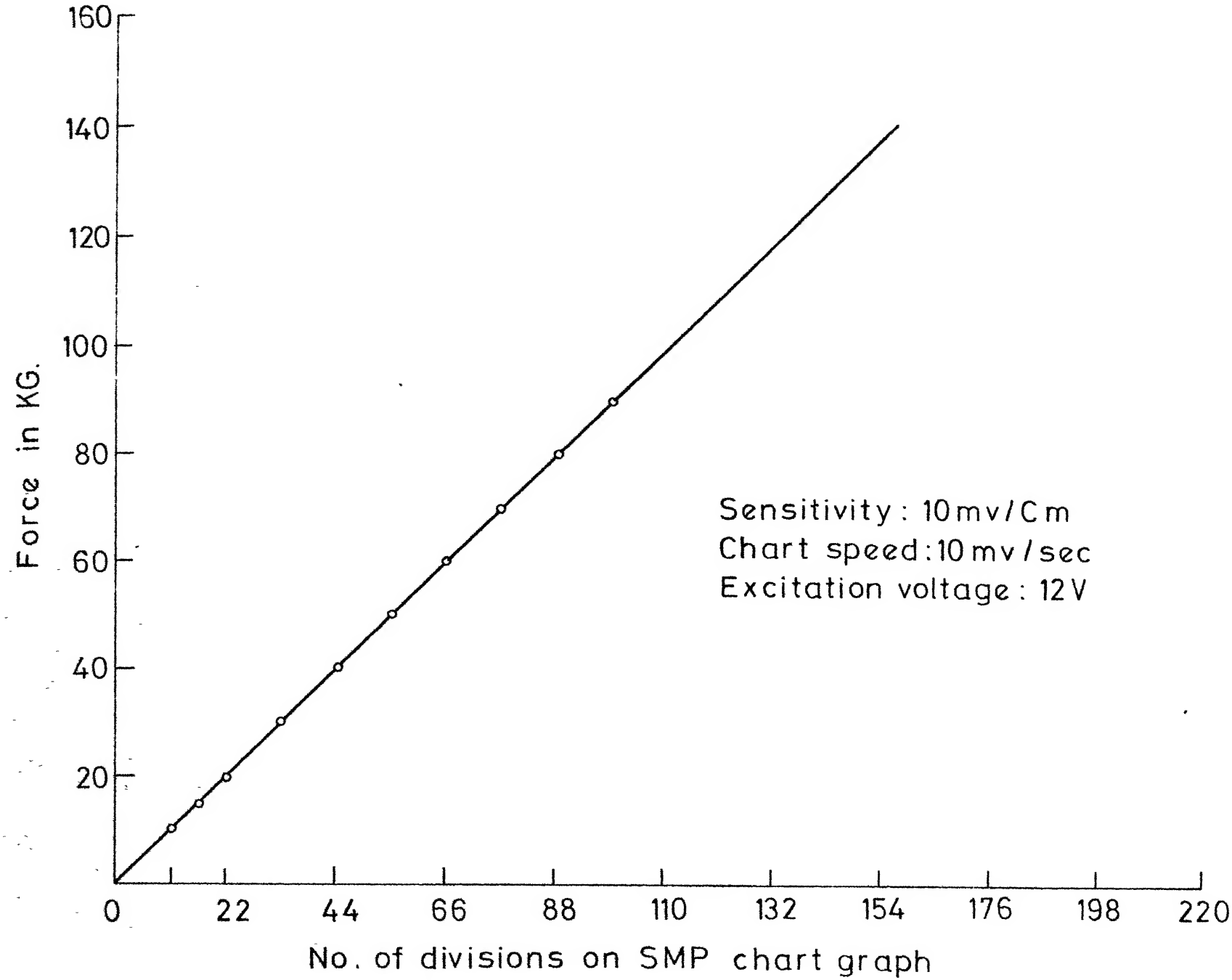

FIG. 2.2 CALIBRATION CHART OF DYNAMOMETER

2.2.2 Die Design Considerations and Specifications:

In the discussion in Section 2.2.1 it was concluded that the straight profiled die would be used. The die is shown in Fig. (1.1). This die has an entry zone, a deformation zone, a bearing zone and an exit zone. The die is a precision tool and hence its profile must be properly controlled to achieve high quality production.

The function of the entry zone is to allow easy flow of lubricant to the die. From this view point, the boundary of the approach cone and drawing cone must be very well blended so that lubricant may be wedged between the die and the wire.

The profile of the drawing cone is most important as the deformation of the wire takes place in this zone. The included angle of the drawing cone depends on the material to be drawn and the percentage reductions taken. Too small an angle brings greater area of wire in contact with the die. The specific pressure is reduced and hence die wear is also reduced. A larger area of contact increases the friction and temperature rise. On the other hand, too large an included angle increases the specific pressure (non-linearly) and causes lubrication failure. This will involve larger wire breaks and cause abnormal die wear.

The bearing zone diameter determines the wire size. Too long a bearing zone will cause excessive friction and lead to wire breaks. Shorter bearings will fail to wipe the lubricant and will allow large quantity of lubricants to pass through the die. This length of bearing varies according to the material being drawn and is defined as percentage of the bore diameter. It is between 0.8 d to 2 d where d is the diameter of the wire.

Keeping all the above factors in mind the die angles and bearing lengths were chosen from Sandvik standard catalogues. Bearing length was chosen as 2 mm.

Semicone angles were chosen as 3°, 4.5°, 6° and 7.5°. The area of reductions were 10% , 15% , 20 % and 25 % . In the industry normally 20% area of reduction is used. The main set of dies which were ordered were of 4.5° semicone angle and 15% area reduction. Following table shows the die numbers, diameter and corresponding variables.

Table 1: Bearing zone length: 2mm, Inlet dia of wire: 2 mm $\pm$ 0.01 mm.

Die No.	Semicone angle (degrees)	Area reduction (Percentage)	Exit diameter (mm)
10 to 19	4.5	15	1.844
20+ to 23	3	15	1.844
30+ to 33	6	15	1.844
40+ to 43	7.5	15	1.844
50+ to 53	4.5	10	1.898
60+ to 63	4.5	20	1.782
70+ to 73	4.5	25	1.734

+ Radio isotope division identification nos. 5653, 5654, 5655, 5656, 5657 and 5658 respectively.

2.2.3 Die Materials

In day to day production Tungsten carbide and diamond dies are used in the industry depending on the type of wire to be drawn. For high r number gauge (smaller diameter) of wire diamond dies are used because they are very small in diameter and low tolerances are easily achieved. But for experimental purposes the use of both the dies was not advisable as longer length of wire had to be drawn to study wear. To start with HSS dies were preferred so that the radioactive technique of study of die wear could be established.

As the present aim is to establish the nuclear technique for the study of die wear, a special type of a HSS containing cobalt was necessary. Super rapid extra HSS has a composition of W = 18% , V = 1% , Cr = 4 % , Co = 5 % and rest iron and carbon. When this material is kept in the reactor all the constituents become radioactive because of nuclear reactions. The half life of all the constituents except Co and Fe is very small. Fe^{59} has a half life of 45 days and cobalt has a half life of 5.3 years. This means that by the time the experiments were performed except cobalt all other constituents of HSS decay to non-radioactive isotopes. Hence this material was chosen. Initially 5 to 10 samples were brought from the market and qualitative analysis was done in the material testing lab.

After confirming the cobalt percentage the material was purchased and was sent to the die manufacturer.

2.3 Selection of Material to be Drawn:

In wire drawing industries different varieties of wire is drawn depending on the requirements of the customer. The criterion for choosing the material for experimental work were easy availability and high wear rates. Keeping the above factors in mind mild steel wire was chosen. It was tested in the material testing lab. for carbon content which was 0.2 percent.

2.4 Experimental Procedure:

2.4.1 Machine Operation:

As discussed earlier in 2.1.1, the wire is pointed using tungsten carbide dies. Wire diameter is reduced to a smaller diameter than the exit diameter of the HSS die. For example, when 1.844 mm exit diameter of the die is to be used for experimentation, the wire has to be pointed to 1.80 mm so that it can pass easily through the die. Gripping of the wire was done by using a pulling dog which was fixed on the capstan. Then the circuit arrangements for dynamometer were made. Initially the capstan was rotated with the hands to keep the wire in tension and motor was started, by using the foot switch while engaging the 2nd gear. 3 to 4 m of wire was drawn on this gear and then gear was changed according to the test requirements.

2.4.2 Nuclear Set-up.

There are various types of radiation detectors to detect the α, β and γ radiations. In the present set-up γ-rays were detected using scintillation detectors. γ-γ coincidence technique was used for measuring the absolute activity. Hence two detectors were necessary. Photograph (2.4) shows the complete set-up. Details of the γ-γ coincidence technique can be found in detail in the earlier work done at this Institute [18,19,20]. Specifications of the present set-up are given in Appendix III.

2.4.3 Sample Making:

Since it was difficult to measure the absolute radioactivity of all the drawn wire, 1 m sections of wire at various lengths were taken for counting. An implicit assumption was made that wire in between two consecutive samples counted will have a proportional amount of die material. Final results were extrapolated accordingly and plotted. 1 m wire was cut into 20 pieces of approximately equal lengths and were put together in a single layer. They were mounted on a perspex sheet with cellotape. Each sample was numbered for identification. The perspex plate was made to slide in the stand made such that the sample was always at the same location with respect to the detectors.

2.5 Measurement of Wear Using Nuclear Techniques:

2.5.1 γ-γ Coincidence Technique:

In application of radiotracer techniques for measuring the absolute wear volumes in the determination of tool wear and grinding wheel loading, several methods were used. Chawla et al. [18] have discussed this at length. The γ-γ coincidence technique was used by Chawla et al., [18,19,20] to study the tool wear and grinding wheel loading. To use this technique a radio-tracer which emits more than one γ-ray is required. Co^{60} is a radiotracer which gives 1.17 and 1.33 MeV γ-rays. This method is more accurate as it eliminates completely the need for explicit considerations of the counting geometry and the efficiency of the detectors in arriving at the absolute wear volumes. In this technique two detectors are necessary to count the two gamma rays. Scintillation detectors are more efficient for measurement of γ-radiations. Hence NaI detectors are used. The two detectors are set in such a way that one detector is sensitive only to radiation of 1.17 MeV and the other only to 1.33 MeV radiation. Absolute activity can be found by using formula,

$$N = C_1 C_2 / C_{12}$$

where, C_1 is the count rate of detector 1, C_2 the count rate of detector 2 and C_{12} the coincidence count rate.

Corrections have to be made for random coincidences and for dead time.

2.5.2 Standardization of Samples:

As discussed earlier HSS dies were manufactured to design specifications and then were sent to BARC for irradiation purposes. Along with the dies small chips of known weights of the same material were also sent. After irradiation they were kept for about 4 months so that the effect of other short lived isotopes except Co^{60} was not significant which assured by taking a γ-spectra of the chip sample. The Ge(Li) spectrum is shown in Fig. 2.3. It is clear from this that there was no significant γ-activity apart from that due to Co^{60}. NaI specimens of the sample are shown in Fig. 2.4. Fig. 2.4(a) is for one detector on which 1.33 MeV γ-ray was set and Fig. 2.4(b) is for another detector on which 1.17 MeV γ-ray was set. By observing both the NaI spectrums, it can be concluded that they have different detector efficiencies. The calculations were made on the area basis and it was found that the error was of the order of 2 % , this discrepancy however does not affect the absolute activity calculations.

Although, the chip samples were of about 0.1gm they were highly active and hence it was difficult to measure the absolute activity by keeping the chip at 3 inches

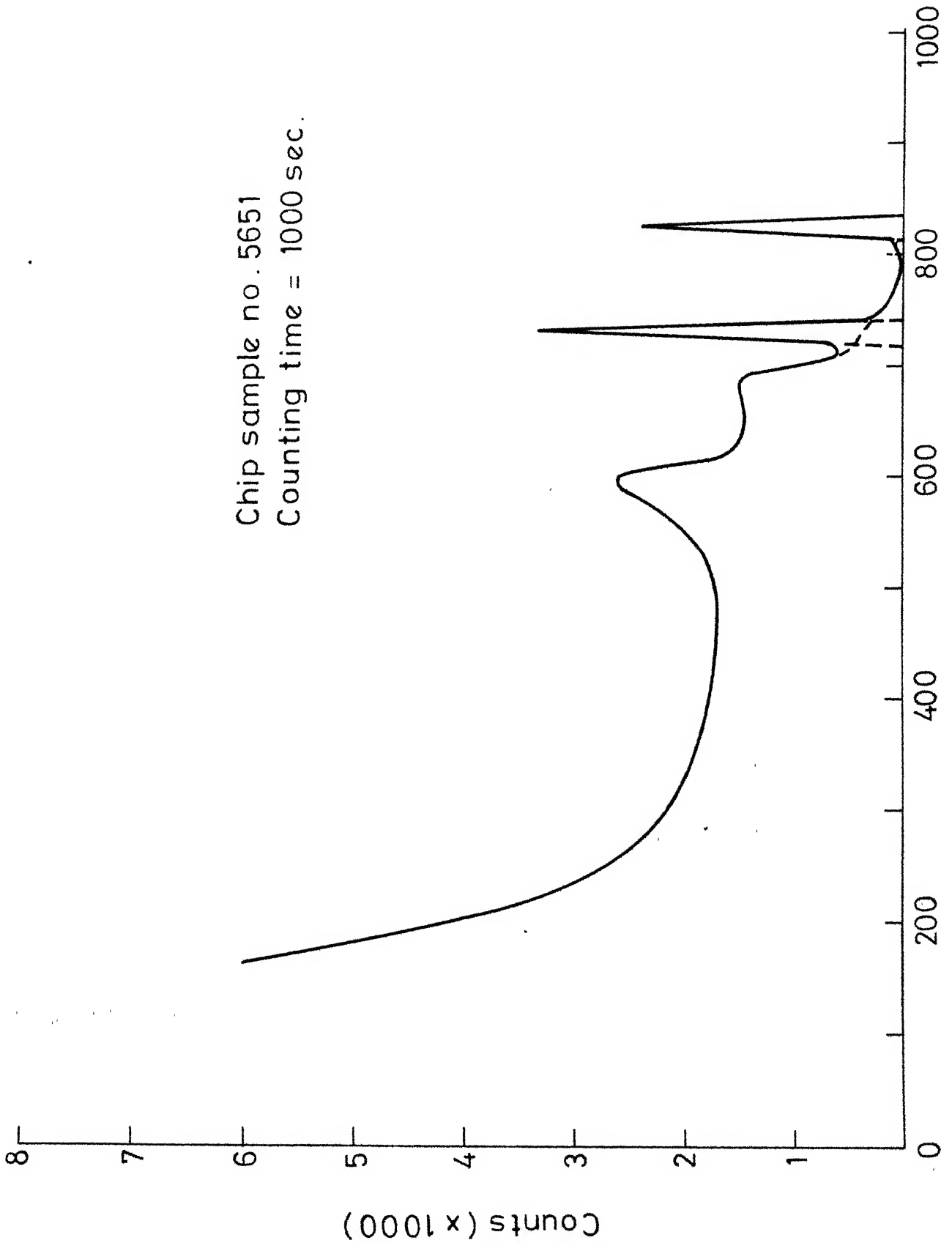

FIG. 2.3 Ge(Li) FULL SPECTRUM OF CHIP SAMPLE

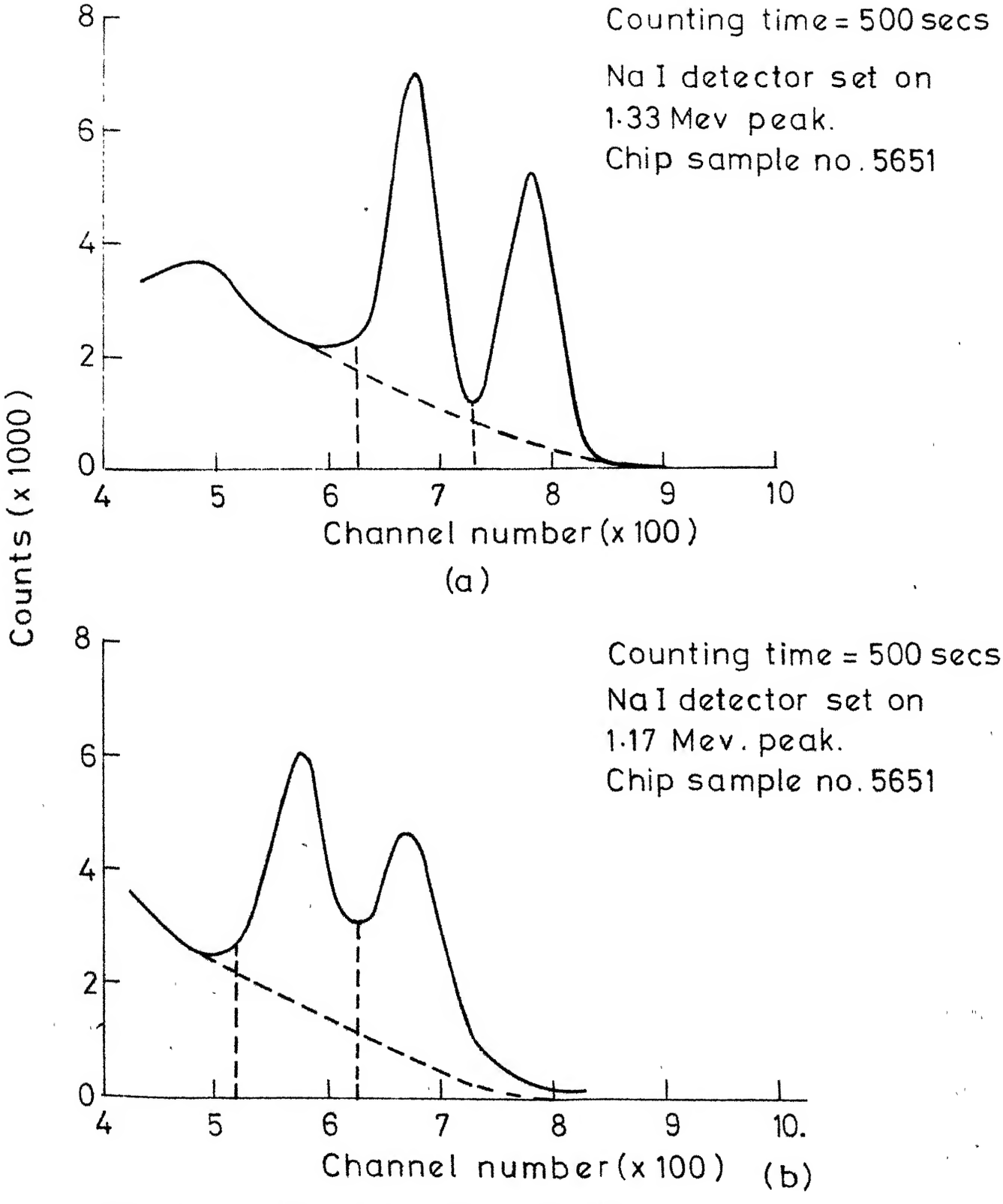

FIG. 2.4 Na I (Th) SPECTRUM

distance from each detector. In this case the dead time corrections were of the order of 75% and random coincidence corrections were also large. This was due to back scatter and lower efficiency of the counter itself for measuring such a higher activity at larger solid angles. Finally the chip was kept at 20 cm and 30 cm from each detector. A standard source 'A' of 10.54 μ Ci (on 1.12.70) was taken and its activity was measured at both the distances. The calculated absolute activity was in agreement with experimental value. In coincidence experiment geometry does not play any role and hence results agreed well for both the distances. The absolute activity of all the chip samples were measured and calculated by using formulas given in Appendix IV. Dead time corrections and Random coincidence corrections were also taken in to consideration. Statistical errors in counting were also calculated by formulas given in Appendix IV. The expected activity by using the formula in Appendix IV was calculated. The following table gives a summary of all the results.

From the table it is seen that expected activity and absolute activity are well with in statistical errors except for 2 values. The two values may be different probably because of the irradiation positions used in CIRUS. In the present work, 5650, 5651 and 5652 dies were used corresponding to die nos. 11, 13 and 15.

Table No. 2

Chip Sample No.	Mass in gms.	Absolute Activity (μ Ci)	Expected Activity(μ Ci)
5650(1)	0.10767	49.21 ± 4.1	47.03
5650(2)	0.10955	54.19 ± 4.51	47.85
5651	0.09075	37.53 ± 2.96	39.64
5652	0.12626	51.54 ± 2.2	55.15
5653	0.09357	47.2 ± 2.95	40.87
5654	0.12441	49.73 ± 4.54	54.34
5655	0.11618	50.94 ± 1.95	50.75
5656	0.14991	66.16 ± 5.2	65.48
5657	0.14021	53.47 ± 2.04	62.05
5658	0.13879	61.14 ± 4.9	60.623

Alongwith the 5650 die 2 chip samples were attached at the entry and the exit to ensure that the activity does not change along the die surface in the drawing direction.

2.5.3 Calibration of Samples:

Samples were prepared as discussed in 2.4.3. The absolute activity of the samples was very low compared to the chip sample. Hence we could not compare and calculate the values directly. The detectors were kept at 3 cm to the sample so that the solid angle made was large. The absolute activity as low as 30×10^{-4} μ Ci was measured.

A weak lab standard source B was taken for relative measurements. The activity of standard source B value was calculated and measured and were found to be same. Standard source A and standard source B were inter-calibrated with the detectors at 3 cm from the source. By knowing the absolute activity of chip material with respect to standard A and sample absolute activity with respect to standard B, the volume of material removed from the particular die can be calculated (since standard A and Standard B are inter-calibrated).

The samples were of very low absolute activity hence the time of counting was taken as 4000 secs. In the case of samples dead time correction and random coincidence corrections were negligible. Error analysis was done by using the formulas in Appendix IV. The results are discussed in the next chapter.

2.6 Measurement of Wear by Conventional Method:

It is very difficult to measure the die wear rate by conventional methods. However, an attempt has been made to measure the volumetric wear by the conventional method and to compare the results with Nuclear results. The die bore and semicone angle were measured on MP-320 projector using incident and transmitted light. A constant magnification factor of 100 was used for all the measurements. The

die exit and entry bore dia were measured and a height gauge was used to measure the deformation zone length and bearing zone length. The volumetric wear can be calculated as follows:

From the Fig. 1.1, the volume V_1 of die bore before wearing out is

$$V_1 = \frac{\pi}{24} [D_b^3 \cot \alpha - D_a^3 \cot \alpha + 6D_a^2 l] \quad (2.4)$$

Let us assume that original diameters D_a and D_b changes to D_a+x and $D_b + x$ after wear respectively, then the volume V_2 of die bore after experiment is,

$$V_2 = \frac{\pi}{24} [(D_b + x)^3 \cot \alpha - (D_a + x)^3 \cot \alpha + 6(D_a + x)^2 l] \quad (2.5)$$

Therefore, the volumetric wear ΔV is,

$$\Delta V = V_2 - V_1$$

$$= \frac{\pi x}{8} [(D_b^2 + xD_b - D_a^2 - xD_a) \cot \alpha + 2(x + 2D_a) l] \quad (2.6)$$

2.7 Evaluation of Frictional Coefficient:

Drawing stress for non work hardening materials can be evaluated using equation 2.2. For strain hardening materials a complex equation needs to be derived. Here only a rough estimate of the frictional coefficient is calculated.

In the above equation all the parameters are known except the coefficient of friction, drawing stress and yield stress of the material. Drawing forces are measured and hence the drawing stress is known. To find the yield stress, mild steel wire used was tested on Instron and stress-strain diagram was plotted. Fig. 2.5 shows the stress-strain diagram. From this figure, it is difficult to find yield stress directly. The yield stress was, therefore, evaluated using the offset method at 0.2 percent strain. By substituting all these parameters in equation 2.2, coefficient of friction was calculated by trial and error.

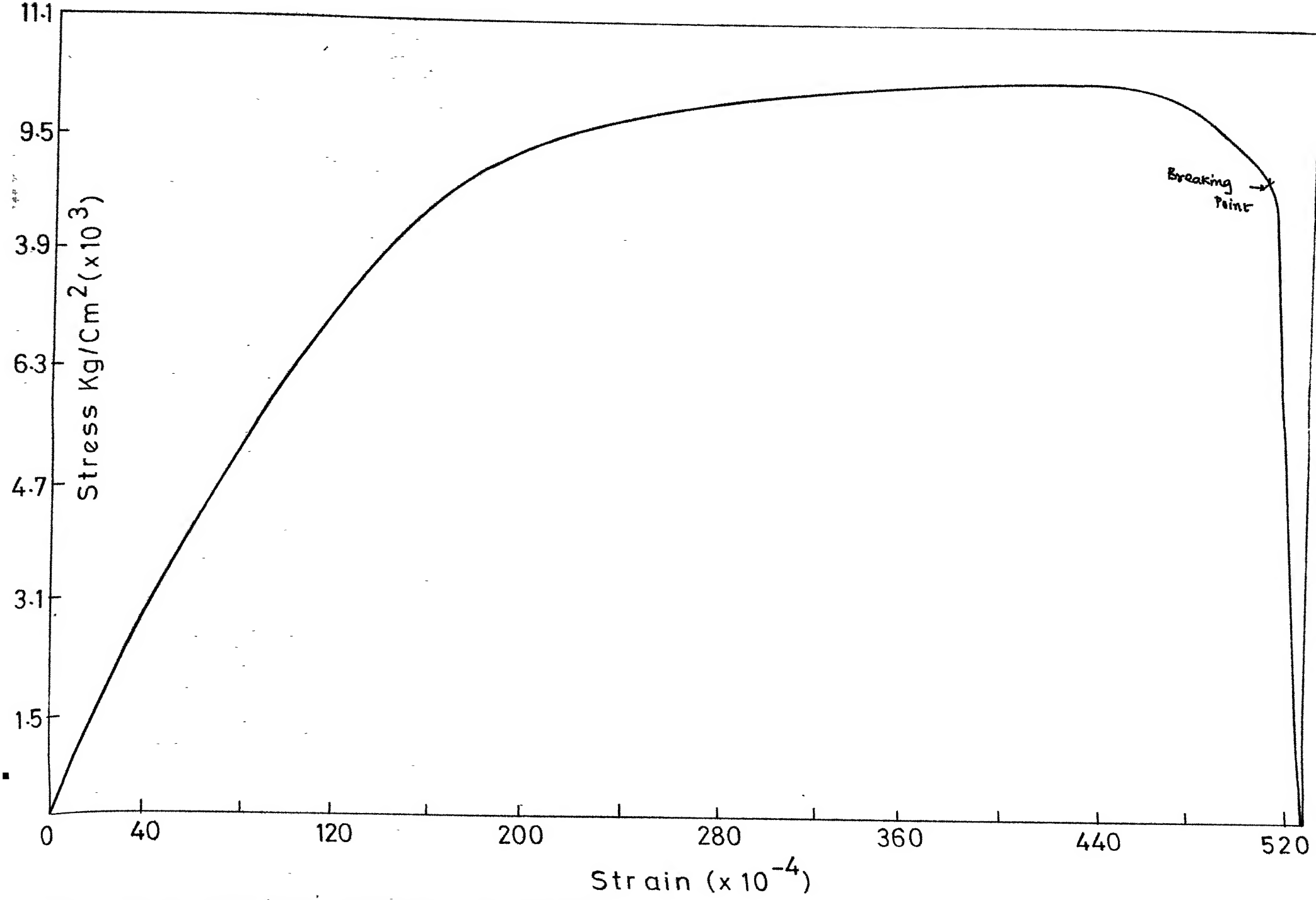

FIG. 2.5 STRESS-STRAIN DIAGRAM

volumetric wear rate curve has reached the steady state. However, on restarting high wear rate similar to one in the initial drawing stages was observed. This indicates that the die life is likely to be more in continuous operation.

As discussed in Chapter I, in wire drawing the wire becomes plastic in the deformation zone and surface temperatures are high. After a certain length of wire has been drawn the temperatures may reach steady state as the wear rate reaches a stable value. Once drawing is stopped the surface temperature of the die will go down. On restarting the drawing before the surface temperature reaches a steady value the wear rate will be high. Hence it is reasonable to expect that the die life will be more in continuous drawing operation in contrast to discontinuous drawing.

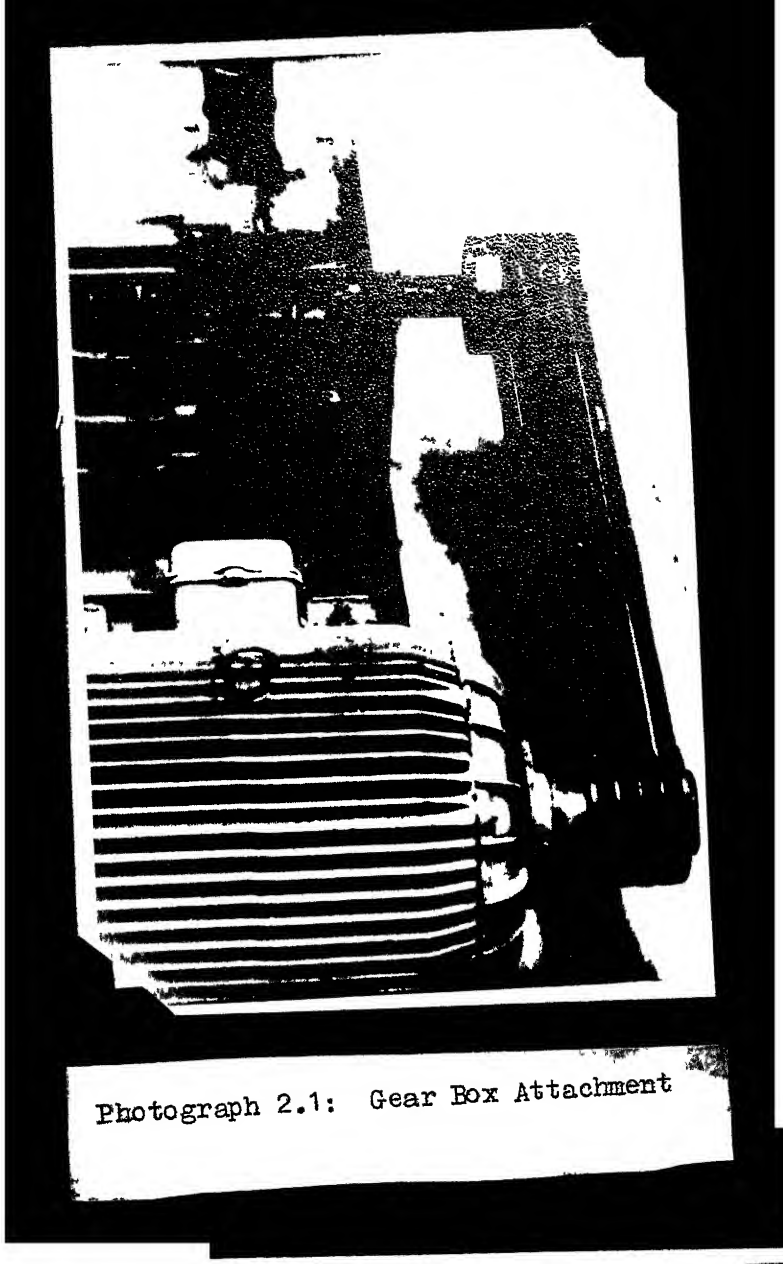

Photograph 2.1: Gear Box Attachment

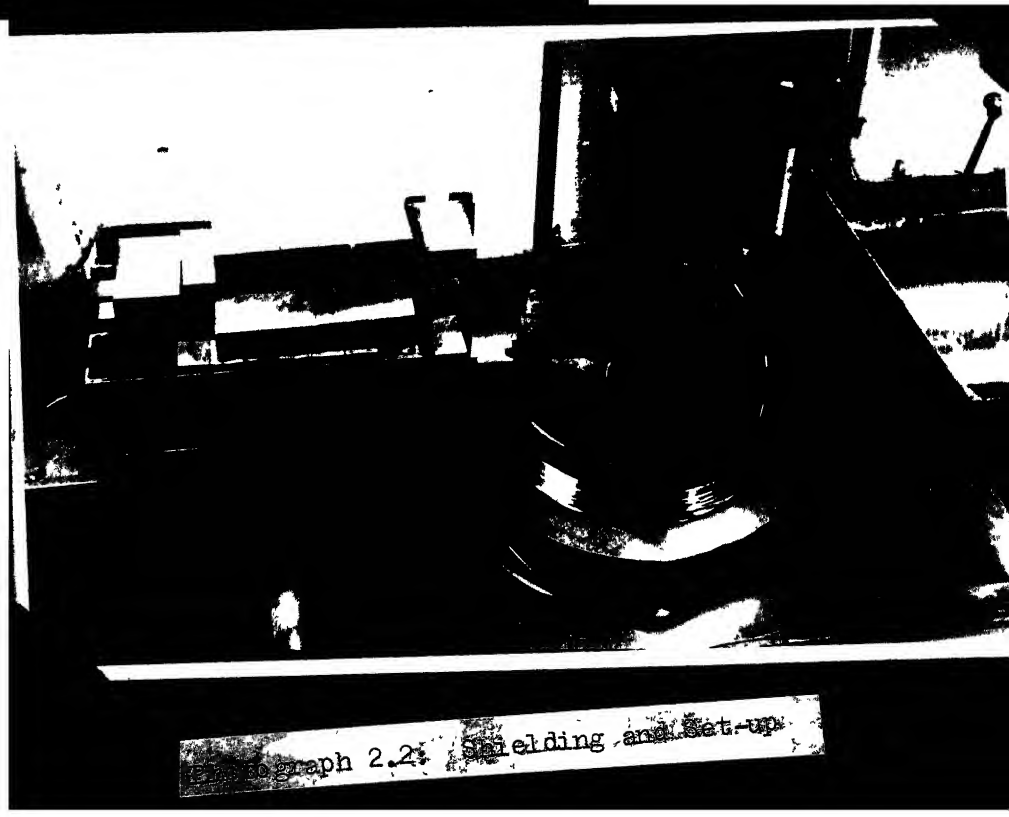

Photograph 2.2: Shielding and Set-up

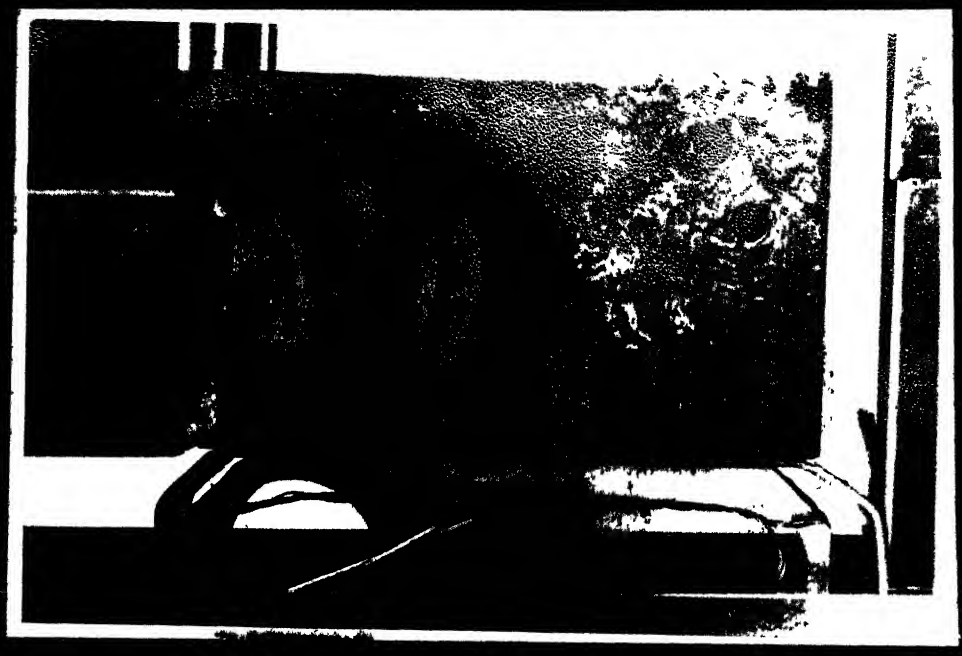

Photograph 2.3: Dynamometer and Die Post Mounting

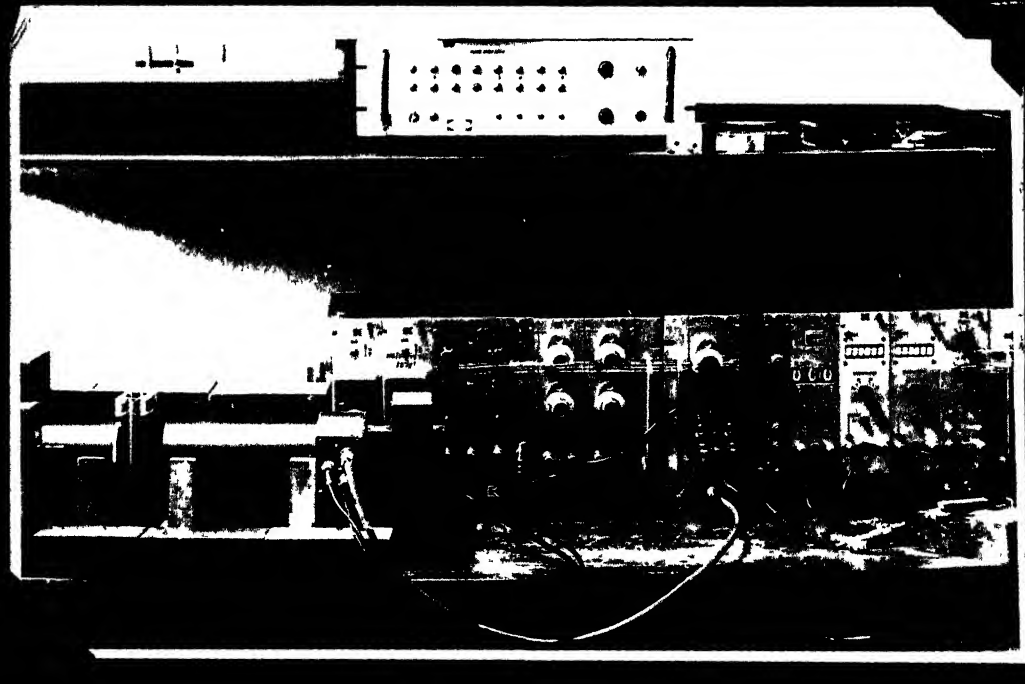

Photograph 2.4: Nuclear Set-up

CHAPTER III

RESULTS AND DISCUSSION

The Nuclear and conventional experiments were performed with different speeds as explained in Chapter II. Conventional experiments were performed with different area of reduction dies and at different speeds (31.77 and 50.09 m/sec.) to make sure that the wire breakage problem would not be there as observed in preliminary experiments. While doing so the following observations were made.

Photograph 3.1 shows the actual bore diameter before the experiment and photograph 3.2 shows the dia bore after performing experiment for 2 minutes 30 seconds at a drawing speed of 50.09 m/sec. and it can be seen from the photographs that there is a change in diameter of the bore. Wear seems uniform around the periphery of the exit hole of the die. The change in diameter was measured and the wear was calculated using equation 2.6. When the conventional volumetric wear values estimated in this way were compared with those obtained by using the nuclear technique, an approximate error of 30 percent was found. This may be because the wear is not constant throughout the length of the die as implicitly assumed in the analysis. It has been found [11] that the wear is generally maximum

at the entry, minimum in the intermediate region and an intermediate value at the exit end. Thus the wear values obtained using equation 2.6 will only provide a rough estimate.

Photograph 3.3 shows the built up edge effect where the material deposition is clearly seen. This experiment was performed at 31.77 m/min. for 1 min 50 secs. While performing the experiment the wire broke suddenly. The die bore was checked and it was found that there was some material deposition. This effect is similar to the phenomenon found in machining. This is mainly due to temperature effects. In Fig. 3.1(a) it has been observed that the drawing forces are very high and hence the value of coefficient of friction will be high resulting in high interface temperature. While wire is passing through the deformation zone it is in the plastic stage and sliding speed is low. Hence the sticking of material to the die is more probable.

The built up edge effect was confirmed while doing the Nuclear experiments. Fig. 3.2(a) gives the volumetric wear curve and Fig. 3.3(a) the inverse wear rate curve. From the V_1 curve in Fig. 3.3(a), it is seen that there is a sudden rise in the inverse of wear. This clearly shows that material deposition has occurred and hence the wear rate has gone down. In the same figure curve V_2 shows the

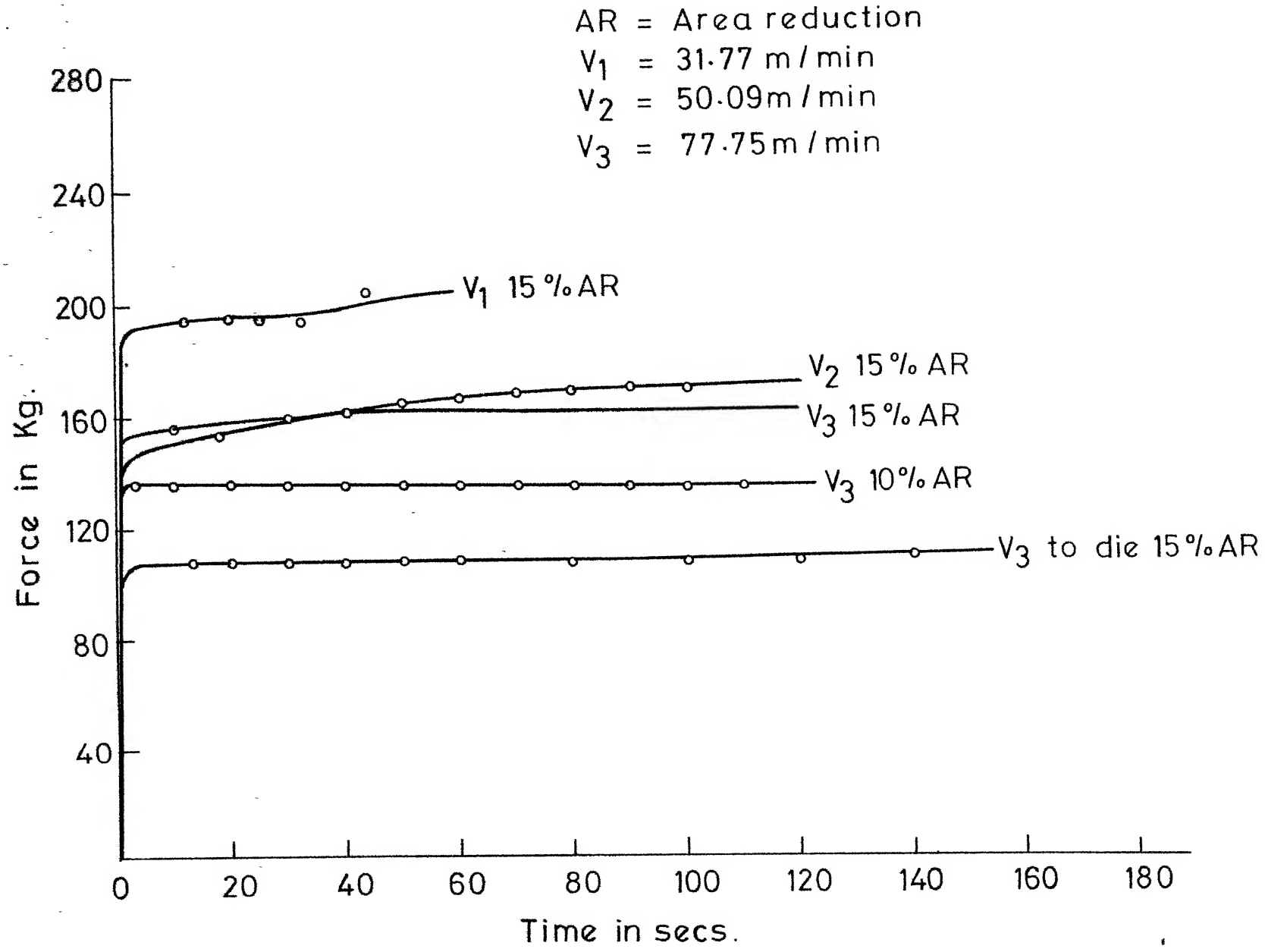

FIG. 3·1(a) DRAWING FORCE VS. TIME

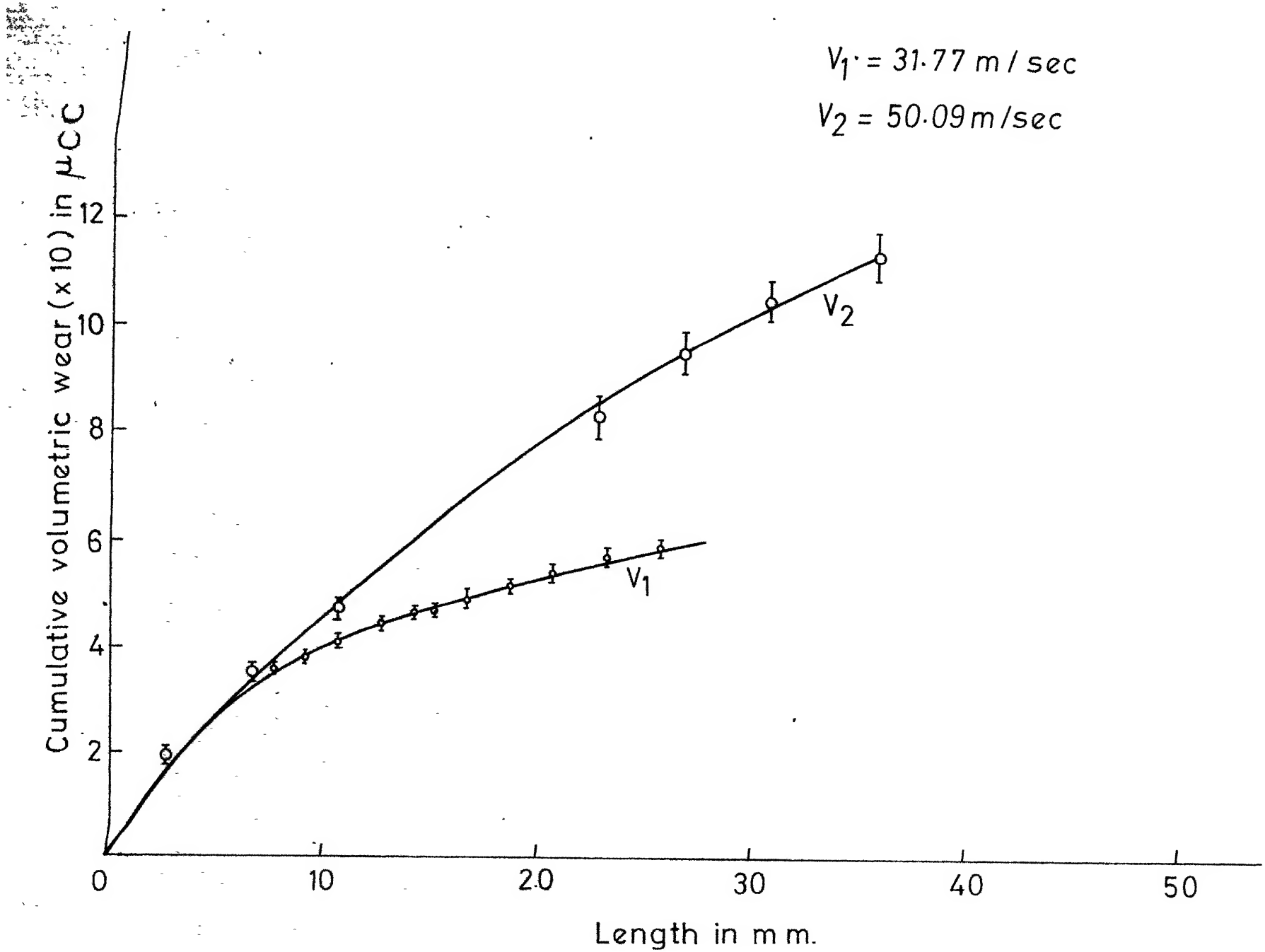

FIG. 3·2 (a) VOLUMETRIC WEAR CURVES

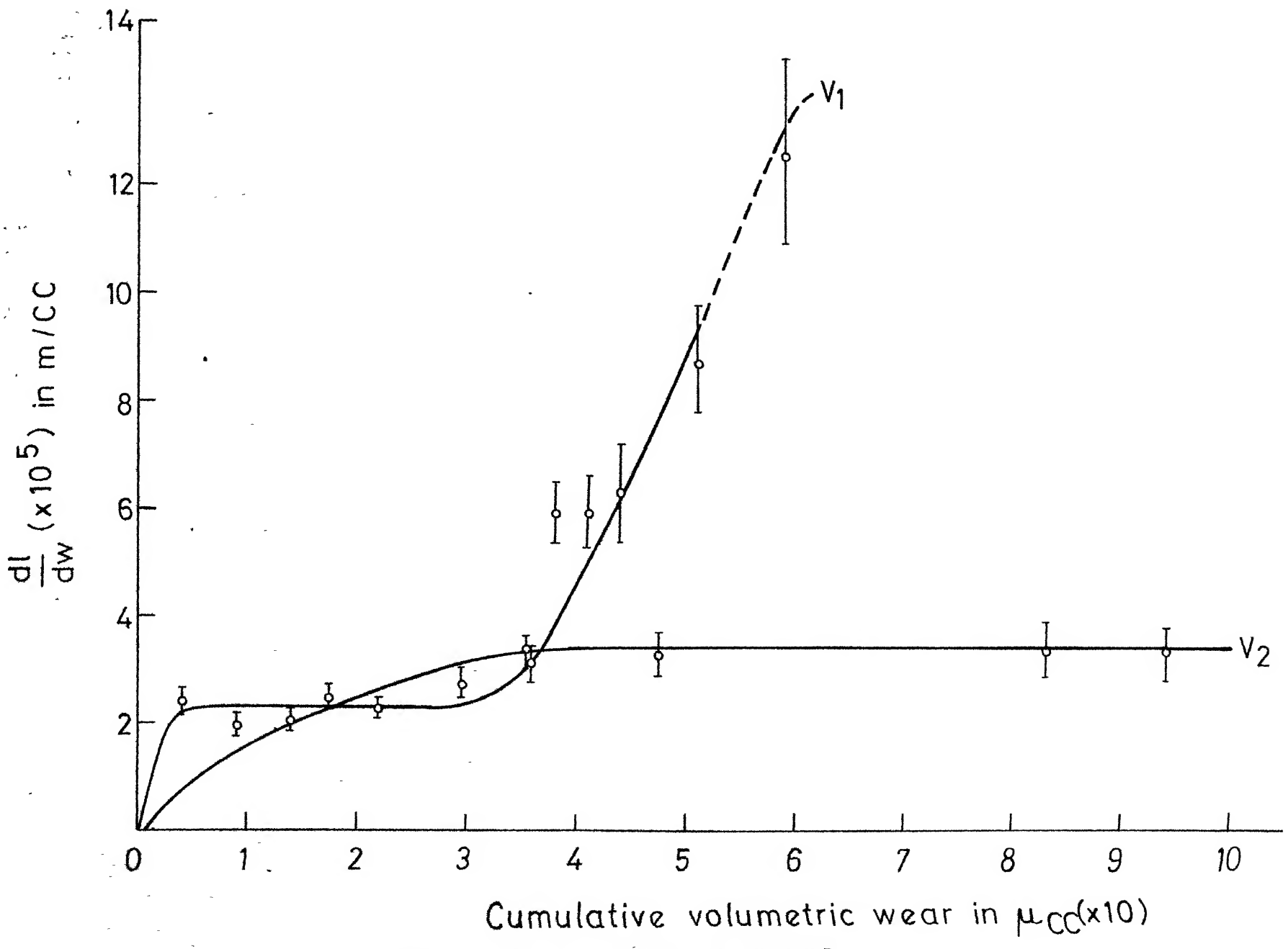

FIG. 3.3(a) INVERCE WEAR RATE CURVES.

steady wear rate. Comparing the two it is apparent that built up edge formation takes place at lower speeds.

Fig.3.1(a) shows the variation in drawing forces. Drawing forces will increase critically as wear rate is high and then they stabilise and increase at a very low uniform rate. The drawing forces are dependent on the value of friction coefficient. This means surface finish of bore is an important factor. Since all the dies have been made by the same manufacturer, it is assumed that they have same surface finish. Making this assumption, from Fig.3.1(a) it is inferred that at lower speeds friction coefficient is high since the forces are high. The values of frictional coefficient were calculated for all the nuclear and conventional experiments using equation 2.6. The table shows the details.

Table 3

Speed m/min.	Area of reduction in percentage	Force Kg	Friction Coefficient μ
31.77	15	204.5	0.37
50.09	15	181.9	0.33
77.75	15	154.5	0.2
77.75	10	136.00	0.17
77.75	15 (Carbide die)	105.5	0.11

from Fig. 3.1(a) it also can be inferred that carbide dies are better than HSS dies as the drawing forces required are less. This implies that frictional coefficient is less which can be seen from the table.

The range of area reduction for the two dies of 1.898 mm and 1.844 mm were 10% and 15% respectively. The difference in the drawing forces for the 2 dies was 24 Kg (138 - 162 Kg). The change in drawing force, therefore, for the 1.844 mm die as its bore increases to 1.852 mm after 2 min. 20 secs. was not measurable by the dynamometer which has a sensitivity of 1 kg for 1 mm at 10 mV/cm. Vibrations inherent in the system and as the feeding spool was lower than the die made the measurement of small force difference difficult.

Fig. 3.2(b) gives the volumetric wear curve for the die which was operated at 50.09 m/min. for 10 minutes. Fig. 3.3(b) gives the inverse wear rate curve. Fig. 3.1(b) gives the force diagram. By comparing Fig. 3.2(b) and Fig. 3.3(b) curves, it is seen that the die had not reached the failure stage. Initially wear increases and then it comes to a steady state and wear rate is constant in that region. To determine the failure zone drawing will have to be done for much longer times. If experiments are done at several speeds it should be possible to establish the die life equation which from the preliminary data collected seems to resemble the tool life curve.

During some experiments, the wire broke after drawing for a fraction of a minute by which time the

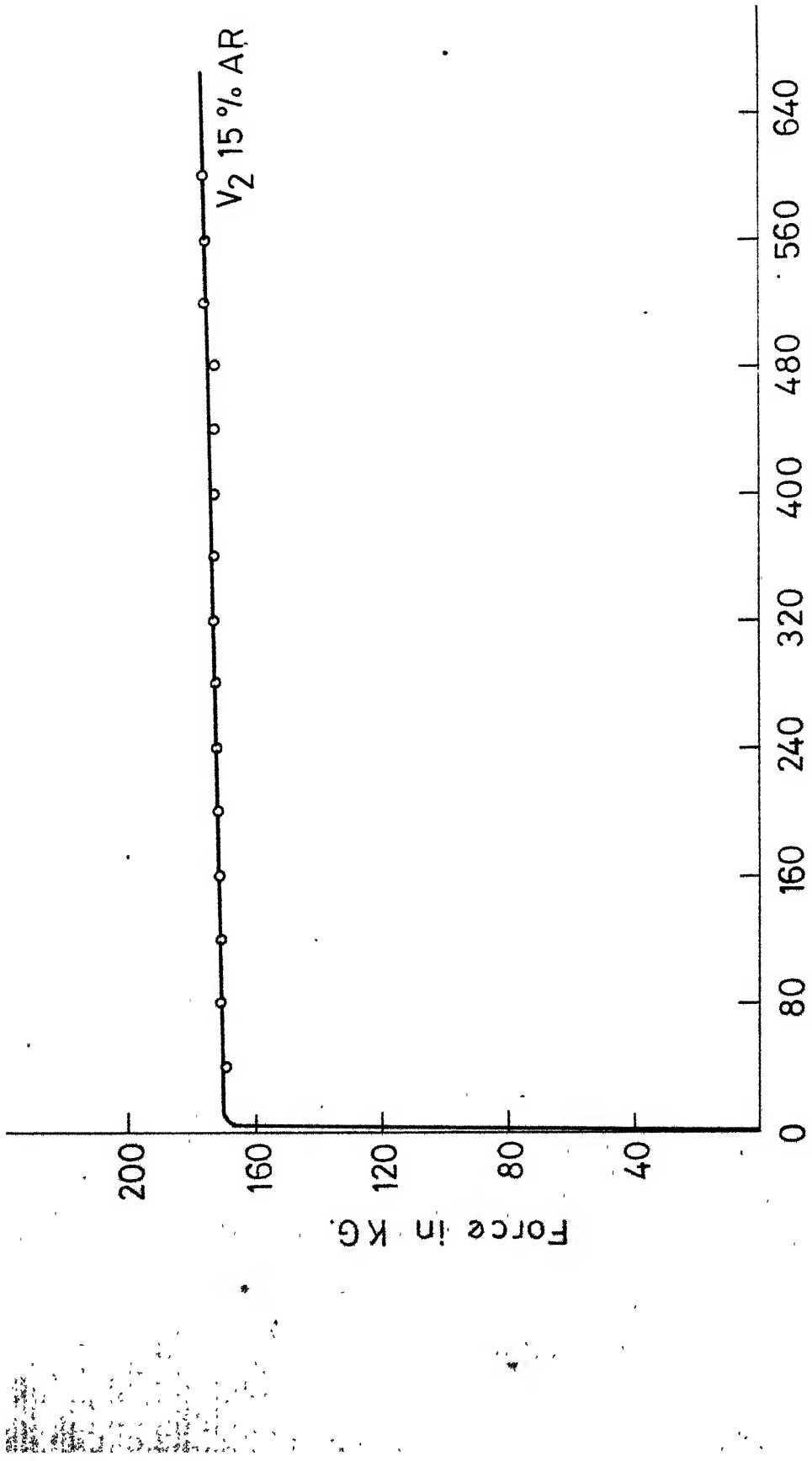

FIG. 3.1(b) DRAWING FORCE VS. TIME

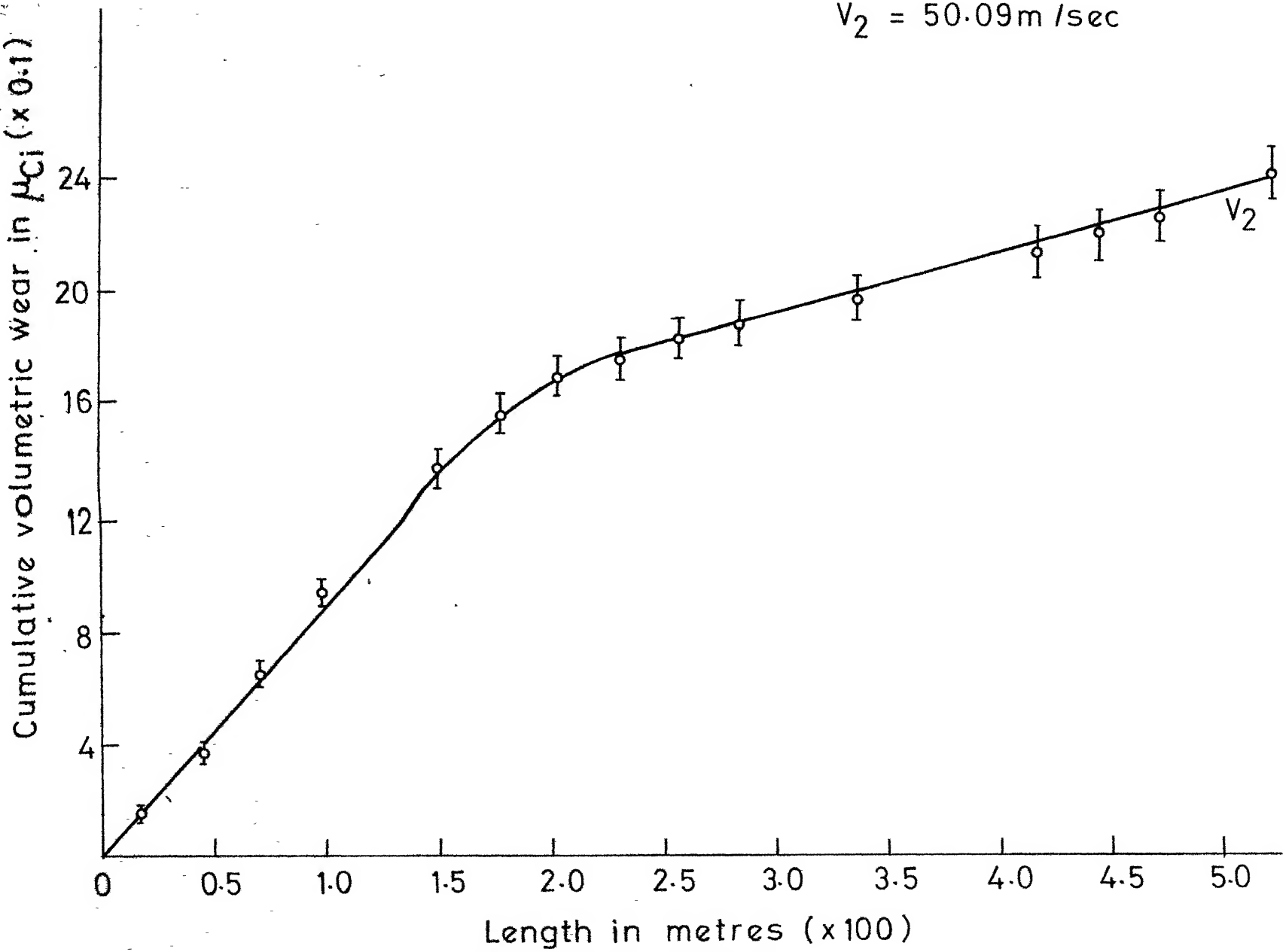

FIG. 3·2 (b) VOLUMETRIC WEAR CURVE

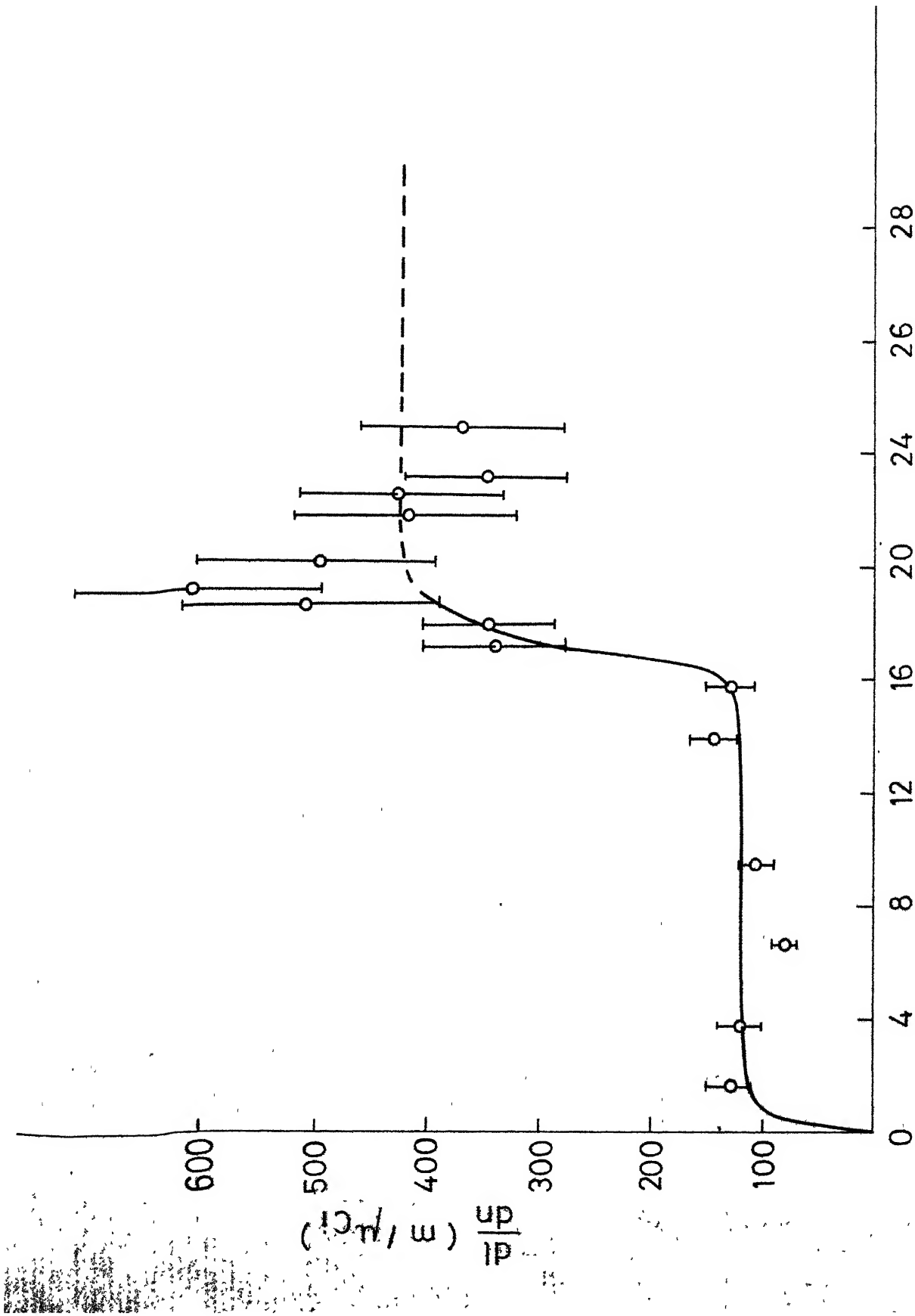

FIG. 3.3(b) INVERCE WEAR RATE CURVE

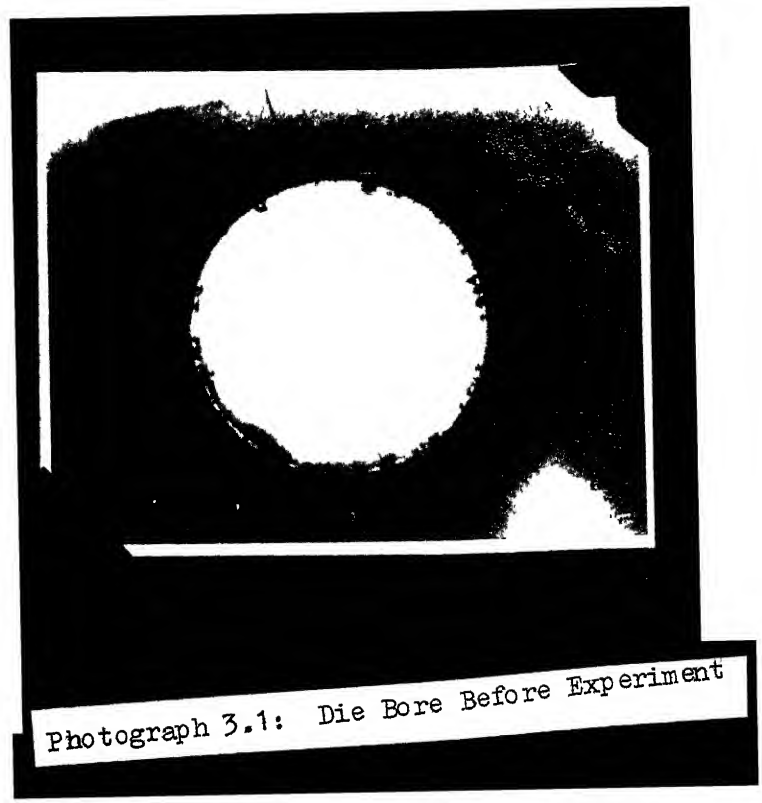

Photograph 3.1: Die Bore Before Experiment

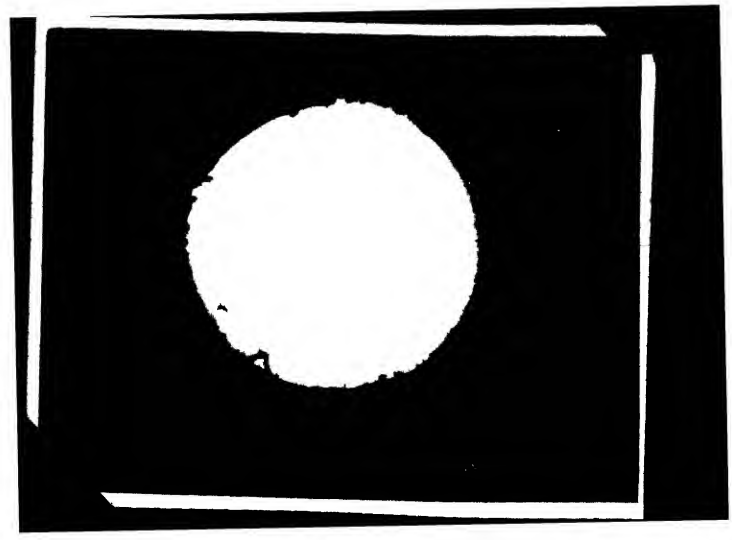

Photograph 3.2: Die Bore After Experiment

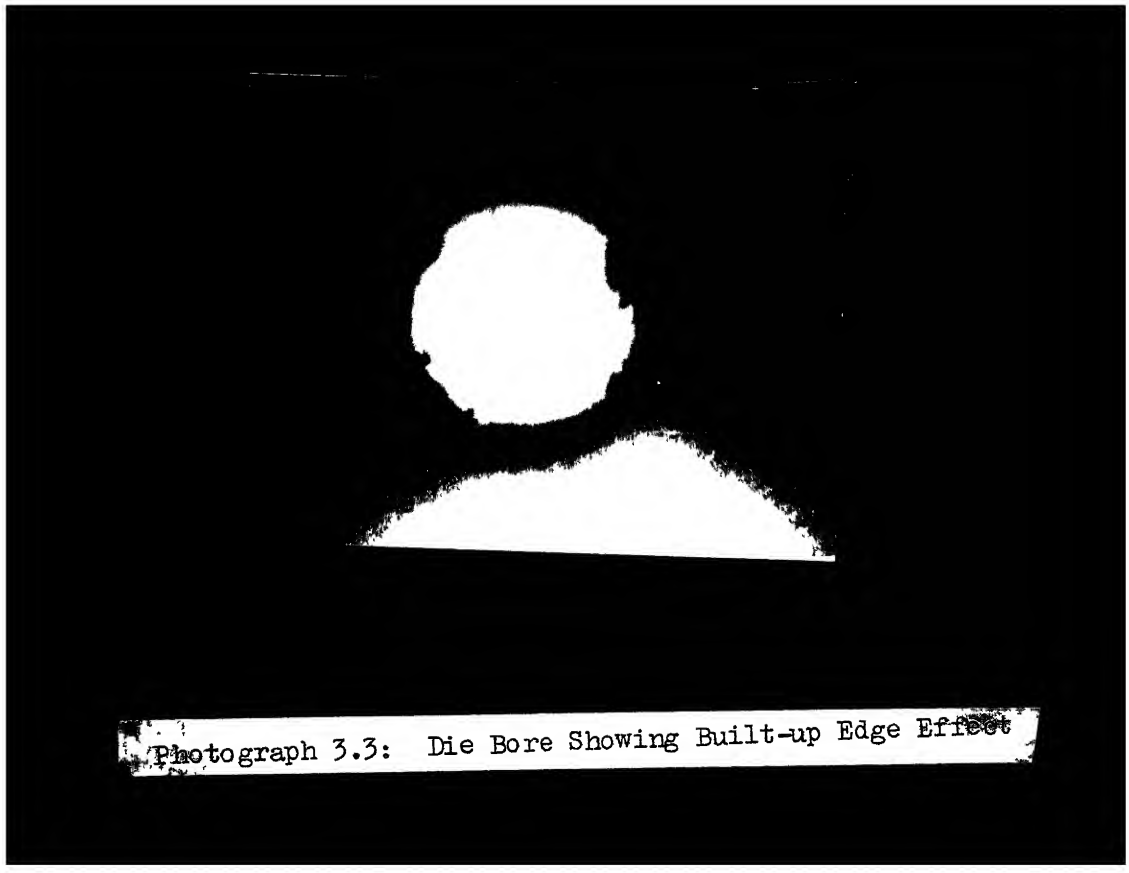

Photograph 3.3: Die Bore Showing Built-up Edge Effect

CHAPTER IV

CONCLUSIONS AND SCOPE FOR FUTURE WORK

4.1 Conclusions:

The γ-γ coincidence technique for absolute wear determination was used by various workers. The efficacy of this technique has been already discussed at length in references [18,19,20]. It was used in the present work and has proved to be a successful technique for the study of die wear in wire drawing.

The built up edge phenomena was observed similar to that which occurs during machining. Experiments indicate that tungsten carbide dies have less friction than HSS dies. Experiments also seem to indicate that die life is likely to be more in continuous operation. The inverse wear rate curves show a resembelance to the cutting tool life inverse wear rate curves [21]. To actually establish the die life equation more experiments varying the different parameters (like speed of drawing, die bore dia, bearing zone length etc.) need to be performed.

4.2 Suggestion for Improvement of the Set-up:

The height of the feeding spool should be kept on line with the die. The difference in height has an effect on die wear. Because they are not on the same level wire

feeding is done at an angle, so there is always a possibility that the die bore will become elleptical. This will also lead to the non-uniform forces on the die surface.

In the force measurement it has been observed that initially within a fraction of a second force rises to a large steady state value about which there are small variations. The force variation can be determined if d.c. output of the strain gauges can be off set to measure variations.

4.3 Scope for Further Work:

In the present work the nuclear technique has been established as a practical method for die wear studies. Further work can be in two directions. First, a study of the effect of varying different parameters like, die semicone angle, area of reduction, bearing zone length, speed of drawing, temperature effects etc. on die wear would be fruitful. Second, the effect on wear for different die and wire materials can be explored.

REFERENCES

1. Buckley, D.H., 'The use of Analytical surface tools in the fundamental study of wear', Proc. Int.Conf. on Wear of Materials, 12, (1977).

2. Hillier, M.J., 'A Hydrodynamic Model of Hydrostatic Extrusion', Int. J. Prod. Res. 5, 171 (1967).

3. Bedi, D.S., 'A Hydrodynamic Model for Wire Drawing', Int. J.Prod. Res. 6, 329 (1968).

4. Wistreich, J.G., 'Investigation of the Mechanism of Wire Drawing', P roc. Inst. Mech. Engg. 169, 659 (1955).

5. Yang, C.T., 'On the Mechanics of Wire Drawing', Trans. ASME, Ser. B 83, 523, (1961).

6. Tegart, W.J.M., 'Elements of Mechanical Metallurgy, MacMillan, New York (1966).

7. Alder, J.F. and Phillips, V.A., 'The Effect of Strain Rate and Temperature on the Resistance of Aluminium, Copper and Steel to Compression', Journal of the Institute of Metals, 83, 80 (1954/55).

8. Jhaveri, K.N.,'Wire Drawing Operation and Associated Problems,' Transaction of a Symposium, Bombay, (1969).

9. Lal, G.K. and Hillier, M.J., 'The Expansion of a Thin Free Tube in Electro-Magnetic Forming', Int. J. Prod. Res. 8, 59, (1970).

10. Sarkar, A.D., 'Wear of Metals', Pergamon, (1976).

11. Wisterich, J.G., 'The Fundamentals of Wire Drawing, Metallurgical Reviews,' 3, 10, 97 (1958).

12. Joul, B.J., 'Study of Die Wear by Means of Radio-Activated Surfaces', Trans. of ASME, 78, 1135, (1956).

13. Button, J.C.E., A.J. Daviss, and R. Tourret, 'A Study of Tracer Methods for Assessing Wear of Wire Drawing Dies', Nucleonics 9(5), 34, (1951).

14. Askouri, M.A., Men, N.S., Ettinger, K.V., Eremlin, J.H., Nowotry, R. and Wills, G.B., 'On line-Wear Monitoring by Surface Activation', Int. J. of Applied Radiations and Isotopes, 26, 61 (1975).

15. Cook, N.H., and East Rabinowicz, 'Physical Measurement and Analysis,' Addison-Wesley, London, (1963).

16. Johnson, W., and Mellor, P.B., 'Plasticity for Mechanical Engineers', Von Nostrand, London (1962).

17. Hu, L.W., 'Analysis of Die Profiles in Wire Drawing', Journal of the Franklin Institute, 263, J. 82, 317 (1957).

18. Chawla, R. and Bhattacharyya, S., 'Determination of Absolute Tool Wear by γ-γ Coincidence Counting of Radiotracers,' Wear, 43, 175 (1977).

19. Chawla, R., and Gohad, A.G., 'Nuclear Techniques for the Quantitative Study of the Loading Phenomenon in Grinding', Int. J. of Applied Radiation and Isotopes, 29, 139 (1978).

20. Chawla, R. and Shah, R.S., 'Evaluation of Wheel Loading in the Grinding of Steels, Brass and Aluminum,' M.Tech. Thesis, IIT Kanpur (1977).

21. Chawla, R., and Datar, S.B., 'Separation of Flank and Crater Contribution to Total Wear in Machining Tests with Radioactive Tools', Proceedings of the 8th AIMTDR Bombay 345, (1978).

22. Donald, D.Glower, 'Experimental Reactor Analysis and Radiation Measurements', McGraw Hill (1965).

APPENDIX I

Wire Drawing Machine Specifications:

Make	:	Wire Machinery Manufacturing Corpn., Ltd., Calcutta
Model	:	WM/400/1, Machine No.: 1088
Drawing speed	:	77.75 m/min. (Capstan Rotating Speed)
Capstan Circumference	:	1.25 m.
Motor	:	SIEMEN Make; 20 HP, 960 rpm.
Capacity of the machine	:	Maximum diameter to be drawn 4 mm (Ferrous) 6 mm (non-ferrous)
Max. tensile load	:	50 Kg/mm^2 (M.S.)

APPENDIX II

Strain Gauge Specifications:

Type	:	Semiconductor
Gauge Factor	:	120
Resistance	:	350 Ohms

Excitation Voltage to be given : 10 to 12 V

Power supply used for exciting the strain gauge : APLAB
Model : LVA 30/0.5

Strip Chart Recorder Specifications:

Make	:	Encardio Rite
Model	:	6320, 2 channel
Sensitivity	:	0.5, 1, 5, 10, 50, 100 and 500 mV/cm, 1 and 5 V/cm.
Chart speed	:	0.5, 2.5, 10 and 25 mm/sec. or m/min.
Sensitivity used for experiments	:	10 mV/cm
Chart speed used for experiments	:	10 mm/sec.

APPENDIX. III

Specifications of the γ-γ Counting Systems:

1. Scintillation Counter Heads:

SH 643 and SH 644 with NaI (TI) crystals of 50 mm x 50 mm size, RCA 8053 photomultipliers, built-in preamplifiers, operating voltage of + 1.0 to 1.5 KV.

2. High Voltage Unit:

Model HV 216, with positive output of 0.5-2.5 KV, a value of 1 KV having been frequently used. High voltage applied: 1000 V.

3. Amplifiers:

Model : PA 521

Attenuation : 20

Gain : 0.1

Time constant : 1 μ sec.

4. Single Channel Analysers:

Model: SC 604 A, Baseline range of 0.2 - 10 V, Window width adjustable between 0 - 2 V.

Setting used : 5.8 to 6.5 V - 1.17 MeV peak

7.2 to 8.1 V - 1.33 MeV peak

5. Coincidence Unit:

Model	:	UC 676 A,
Resolving time	:	0.1 - 2 μ sec. on one of the input channels
Resolving time used	:	200 η sec.

6. Timer:

Model	:	E T 5300

7. Scalars:

Model	:	E C 5101
	:	DS 328 A (for coincidence unit)

APPENDIX IV

ACTIVITY CALCULATIONS AND ERROR ANALYSIS

Calculation of Activity Expected:

$$\text{Expected activity} = \frac{\sigma_a \, \phi \, NV(1-e^{-\lambda tr}) \, e^{-\lambda t}}{3.7 \times 10^{10}} \text{ Ci}$$

where tr : irradiation time in days

t : time of observation in days after irradiation

$1/\lambda$: mean life of Co^{60} in days

ϕ : irradiation flux in neutrons/cm^2-sec.

σ_a : microscopic neutron absorption cross-section of Co^{59} in cm^2

N : atom density of Co^{59} in atoms/cm^3

V : Volume of iron in cm^3

Because tr = 1 day and t ~ 120 days, the above expression can be approximated as:

$$\text{expected activity} = \frac{N\sigma_a \, \phi \, V \lambda \, tr}{3.7 \times 10^{10}} \text{ Ci}$$

where σ_a : 17×10^{-24} cm^2

ϕ : 5×10^{12} neutrons/cm^2-sec.

NV : $\frac{\text{Mass of } Co^{59} \text{ in sample} \times 6.023 \times 10^{23}}{59}$

λ : $\frac{0.693}{T_{1/2}}$,

where $T_{1/2}$ = 5.3 years.

Calculation of Absolute Activity:

$$\text{Activity: } N = \frac{C_1 C_2}{C_{12}} \times \frac{1}{3.7 \times 10^{10}} \text{ Ci}$$

where C_1 is the count rate of channel A, C_2 the count rate of channel B and C_{12} the coincidence count rate.

Dead time Correction

$$\text{Dead Time: } \tau = \frac{N_{01} + N_{02} - N_{012} - N_b}{N_{012}^2 - N_{01}^2 - N_{02}^2}$$

where N_{01}, N_{02} are the count rates of two individual sources, N_{012} the count rate of two sources together and N_b the background count rate.

$$N_t \text{ (True count rate)} = \frac{N_0}{1-N_0 \tau}$$

Random Coincidence: $R = 2\tau C_1 C_2$

where τ is the coincidence unit's resolving time.

Error Analysis:

$$AVA = \frac{A_1+A_2+\ldots A_n}{n}$$

where A_1, A_2,..., A_n are set of count rate readings in channel A.

$$\text{ERR A} = \left(\frac{AVA}{n} + \text{Back A} \right)^{1/2}$$

where ERRA is the Error and Back A is the Background count rate.

Similarly for channel B and coincidence unit,

ERR B and ERR AB can be calculated respectively.

$$SIG = [(AVA - BACK\ A) \times ERR\ A]^2 + [(AVB - BACK\ B) \times ERR\ B]^2$$

$$ERAC = [(AVA-BACK\ A) \times (AVB - BACK\ B) \times ERR\ AB]^2 + AVAB^2 \times SIG$$

$$ERRAC = [ERAC/AVAB^4]^{1/2}/(3.7 \times 10^{10})$$

where ERRAC is the final error in the activity

$$ERRW = [SQRT\ (ERAC/[(AVA-BACK\ A)(AVB - BACK\ B)]^4)] \times 3.7 \times 10^{10}$$

where ERRW is error in the inverse wear rate.

Cumulative Error Calculations:

l_i = length of the wire

N_i = Activity

σ_i = ERROR

f = factor = $(l_{i+1} - l_i - 1)/2$

Cumulative activity = $NC\ (i+1) = N_i + (N_i + N_{i+1})\ f + N_{i+1}$

Cumulative activity error

$$= \sigma_{c(i+1)} = [\sigma_i^2 + (\sigma_i^2 + \sigma_{i+1}^2)\ f^2 + \sigma_{i+1}^2]^{1/2}$$

A 58355

Date Slip

This book is to be returned on the date last stamped.

CD 6.72.9

ME-1979-M-JAJ-EVA